Clim. Past Discuss., 3, 899–933, 2007
www.clim-past-discuss.net/3/899/2007/

Climate of the Past Discussions

Climate of the Past Discussions is the access reviewed discussion forum of *Climate of the Past*

Non-linear statistical downscaling of present and LGM precipitation and temperatures over Europe

M. Vrac, D. Paillard, and P. Naveau

Laboratoire des Sciences du Climat et de l'Environnement, LSCE, CEA/CNRS/UVSQ, Institut Pierre Simon Laplace (IPSL), Centre d'étude de Saclay, Orme des Merisiers, 91191 Gif-Sur-Yvette, France

Received: 20 June 2007 – Accepted: 20 June 2007 – Published: 6 July 2007

Correspondence to: M. Vrac (mathieu.vrac@lsce.ipsl.fr)

Abstract

The needs of small-scale climate information have become prevalent to study the impacts of future climate change as well as for paleoclimate researches where the reconstructions from proxies are obviously local. In this study we develop a non-linear statistical downscaling method to generate local temperatures and precipitation values from large-scale variables (e.g. Global Circulation Model – GCM – outputs), through Generalized Additive Models (GAMs) calibrated on the present Western Europe climate. First, various monthly GAMs (i.e. one model for each month) are tested for preliminary analysis. Then, annual GAMs (i.e. one model for the 12 months altogether) are developed and tailored for two sets of predictors (geographical and physical) to downscale local temperatures and precipitation.

As an evaluation of our approach under large-scale conditions different from present Western Europe, projections are realized (1) for present North America and Northern Europe and compared to local observations (spatial test); and (2) for the Last Glacial Maximum (LGM) period, and compared to local reconstructions and GCMs outputs (temporal test).

In general, both spatial and temporal evaluations indicate that the GAMs are flexible and efficient tools to capture and downscale non-linearities between large- and local-scale variables. More precisely, the results emphasize that, while physical predictors alone are not capable of downscaling realistic values when applied to climate strongly different from the one used for calibration, the inclusion of geographical-type variables – such as altitude, advective continentality and W-slope – into GAM predictors brings robustness and improvement to the method and its local projections.

1 Introduction

Understanding the present climate and its changes is a difficult challenge. One basis of such a research lies on studies of the long past climate history. To perform such a task at a global scale, useful devices are the well-known General Circulation Models (GCM), complex computer codes simulating the atmospheric circulation through resolving the equations of the world atmospheric dynamics, often coupled with oceanic models to take into account the interactions between the oceans and the atmosphere. Although these numerical tools are required to get a global understanding of the land-ocean-atmosphere system, they are computationally intensive and, then, can only produce relatively low spatial resolution simulations. Consequently, they do not capture small-scale physical processes which drive some important local surface variables and their high-resolution properties, such as precipitation (occurrence and intensity) and its strong spatial variability (e.g. Wood et al., 2004). This is particularly true for paleo studies, often requiring very low resolution GCMs to be able to simulate climate over thousands of years (e.g. Rahmstorf and Ganopolski, 1999). Due to these low resolutions, model outputs are difficult to compare to local present observations (e.g. Vrac et al., 2007a) and even more to extreme climate events (e.g. Vrac and Naveau, 2007) or local climate reconstructions from proxies (e.g. Kageyama et al., 2006). However, these comparisons are essential to assess regional impacts of future climate change needed at regional scales, or to understand physical, chemical or biological mechanisms at lower scales in many present, near-present (past or future) and (long term) paleo-climate studies.

In order to overcome these scale issues, it is necessary to develop *downscaling* methods to generate realistic local time series from large-scale model outputs. Regional Climate Models (RCMs) are a first approach. They can be understood as *regional* GCMs, i.e., models solving the equations of the smaller scale (5 to 50 km) atmosphere dynamics for given regions (e.g. Liang et al., 2006). However, because these models are equally (if not more) computationally intensive than GCMs in generating local or regional variables, an other approach has recently received an outburst of interest: the statistical downscaling methods (SDMs).

As indicated by their name, these methods rely on modeling statistical relationships between local-scale data (e.g. observations, reconstructions) and large-scale upper-air

CPD

3, 899–933, 2007

Non-linear statistical downscaling over Europe

M. Vrac et al.

EGU

atmospheric variables (e.g. reanalysis data, GCM outputs). Different statistical models have been developed in this goal, usually classified into three (sometimes overlapping) families of methods: transfer functions (e.g. Zorita and von Storch, 1998; Sell et al., 2000; Huth, 2002), weather typing (e.g. Bardossy et al., 1994; Huth, 2001; Vrac et al., 2007a) and weather generators (e.g. Wilks, 1999; Wilks and Wilby, 1999). In contrast to RCMs, because of their (generally) weak computational requirements, the SDMs are fast in simulating local climate variables and they allow modeling the associated uncertainties more easily than with RCMs (e.g. Katz, 2002). However, in context of changing large-scale climate conditions, SDMs can have troubles to generate evolving local climate variables. Indeed, by construction, many SDMs assume that the modeled connections (large vs. local scales) are linear and remain the same in different climate (e.g. Wilby et al., 1998; Vrac et al., 2007b[1]). This can lead to unrealistic future or past statistical relationships and then to unrealistic projections of local variables. This difficulty is emphasized in a framework of long past studies, as in paleoclimate downscaling. Hence, it is necessary to develop *nonlinear* and *robust* models under strong climate change.

The statistical model that we propose in this article aims at responding to these needs with the downscaling of precipitation and temperatures for the Last Glacial Maximum (LGM) period. First, it brings the necessary flexibility to represent the large- vs. local-scale relationships with strong nonlinearities when needed. Second, it incorporates physical as well as geographical variables to gain robustness in the downscaling projections under changed climate conditions.

The rest of this article is organized as follows. In Sect. 2, the large and regional-scale data used are presented. Then the proposed statistical model is developed and an application is performed and presented in Sect. 3. Conclusions and a short discussion are provided in the last Sect. 4.

[1] Vrac, M., Stein, M., Hayhoe, K., and Liang, X. L.: A general method for validating statistical downscaling methods under future climate change, Geophys. Res. Lett., submitted, 2007b.

2 The large- and local-scale data and the statistical method

To calibrate any SDM, two types of data are required: large-scale and local- or regional-scale data. The small scale data must be at the desired resolution for local projections and the large-scale data at the same resolution as the data used to drive the projections. In this article, the region of study corresponds to Western Europe. Hence, each type of data covers approximately the geographical rectangle [10° E; 20° W] × [37° N; 55° N]. This region has been choosen because it contains various physical and geographical contrasted conditions. Oceanic influences (e.g. Atlantic, North Sea), high mountains near the center (Alps, Pyrenees), Mediterranean conditions, and continental climate (eastern countries) imply a large range of local temperatures and precipitation values and large-scale variables. This large range is a necessary condition to efficiently calibrate our method for a present climate and applying it under evolving conditions.

2.1 Large-scale data: the climber model

The large-scale data used in this work are outputs from the CLIMBER model (Petoukhov et al., 2000) that has a large spatial resolution of 10° in latitude and 51° in longitude. It is an intermediate complexity model, in comparison to 3-D general circulation models, it includes less explicit representations of atmospheric features, thus relying on more parameterizations. In particular, it doesn't compute explicitly the atmosphere dynamics at the synoptic scales but accounts for their effects on the meridional heat transport. Thus, it ignores the variability at the daily time scale of meteorological events (e.g. winds associated with low pressure systems) and also at the time scale of a few years, in particular the North Atlantic Oscillation.

The CLIMBER model has been conceived to allow for very long (10^3 to 10^6 years) or a large number of integrations. Thus, it is a suitable tool for the paleoclimate community or for long future time projections. Despite its simplicity, CLIMBER was favorably compared to results from more complex models, both in a paleoclimate framework (Kageyama et al., 2001) as well as in an upcoming global warming context (Pethoukhov

CPD

3, 899–933, 2007

Non-linear statistical downscaling over Europe

M. Vrac et al.

EGU

et al., 2005). Nevertheless, it is crucial to keep in mind that CLIMBER simulates the atmosphere, the ocean and the vegetation. Then, the obtained results largely depend on other components of the climate system, notably on the ice sheets and the carbon cycle, that are prescribed in the model. However, the understanding of the past evolution of atmospheric CO_2 is still fragmentary, future projections are then not much constrained yet. It is, overall, in these boundary conditions imposed to CLIMBER that the largest uncertainties on the future climate evolution are located.

2.2 Regional-scale data: the CRU climatology

The regional-scale temperature and precipitation data used for calibration and validation of our statistical model, come from the "Climate Research Unit" database (CRU, New et al., 2000). These regularly gridded data were chosen because of their global land covering at the high spatial resolution of 10' (i.e. 1/6 degree) and because of their monthly temporal resolution that is consistent with the CLIMBER temporal resolution.

The CRU database corresponds to a monthly present *climatology*. That means that for each grid-point and each available variable (here, temperatures and precipitation), we have 12 mean monthly values which are representative of the actual climate. In addition, CRU provides us with the mean altitude of each grid-point.

2.3 The statistical method: generalized additive models

Our goal is here to develop a statistical model capable of regressing the values of variables Y (temperature and precipitation), called *predictands* – i.e. values to be predicted – taken from the CRU database. The *predictors* X_j – i.e. the variables used to predict Y – are values derived from CLIMBER outputs (see next Section). Based on our goal of developing a non-linear method that is robust under evolving climate, the choice of available approaches is reduced. The statistical approach retained is a Generalized Additive Model (GAM, Hastie and Tibshirani, 1990). An advantage of this method is that it allows visualizing the relationships between the predictands and the predictors through non-linear and non-parametrical functions. Indeed, GAM models the predictands Y (i.e. CRU data) as a sum of spline functions (e.g. de Boor, 2001) f_j applied to different predictors X_j:

$$Y = \sum_{j=1}^{p} f_j\left(X_j\right) + \varepsilon. \tag{1}$$

This model corresponds to a non-linear regression between large and smaller scale. Splines are piecewise parametrical or non-parametrical functions. That means that for each piece, a function (of a given form) is estimated. For example, if the chosen form is a second order polynomial function and that three intervals (i.e. pieces) are selected, the associated spline function corresponds to three second order polynomial functions. Consequently, a spline is a non-linear component of Y according to each predictor. In this work, the chosen splines are piecewise third order polynomial functions.

The ε term of equation (1) is the model error that is supposed to be normally distributed with zero mean (Hastie and Tibshirani, 1990). Cumulated precipitation data can generally be correctly modeled according to log-normal distributions. Hence, to be in agreement with the statistical theory of GAM, in the following, for the precipitation data, the Y variables will correspond to the log-values of the CRU precipitation intensities. Temperature data, being generally Gaussian, will be provided to GAM without transformation.

As an illustration of the ability of GAM to model linear and/or non-linear relationships when needed, Fig. 1 shows the spline functionsf_j estimated for a toy model calibrated for July local precipitation data with four predictors being specific humidity (Q), wind intensity in the v direction (Wv), the altitude (elv), and latitude (LAT). More details about the data will be provided in Sect. 3.1. In this figure, the x-axes correspond to the predictors data, and the y-axes to their contribution in the modelling of Y. This example corresponds to $p = 4$ functions f_j in relation (1). These four panels indicate that while the contributions from Q and Wv are modeled through strong non-linearity, elv and LAT contributions are mostly linear, and the LAT spline is clearly uninformative in this toy model for precipitation.

3 Applications and results

3.1 The predictor variables

In this article, because of their availability and supposed links to the variables to be downscaled, 15 predictors are chosen as potential informative candidates for explaining Y:
– Nine "physical" variables:

- specific (Q) and relative (RH) humidity,
- sea level pressure (SLP),
- temperature (T),
- wind intensity in u (Wu) and v (Wv) directions,
- dew point temperature(Td),
- dew point temperature depression DTd = Td – T,

DTd represents the degree of saturation in water vapor of the atmosphere. Td and DTd have shown good capacities of prediction for downscaling of precipitation (Charles et al., 1999; Vrac et al., 2007a, Vrac and Naveau, 2007),

- vertically integrated specific humidity (QI).

– Six "geographical" variables:

- longitude (LON) and latitude (LAT),
- elevation (elv),

– advective (Aco) and diffusive (Dco) continentality (see definition below),

– W-slope (Wsl) (see definition below).

The diffusive continentality index Dco (between 0 and 1) corresponds to the shortest distance to the ocean. The closer a point to a sea or an ocean, the closer the index to 0. Conversely, the further a point from the sea, the closer the index to 1.

The advective continentality Aco (between 0 and 1) is associated to wind intensities and directions at the point considered. It is based on the following hypothesis: an air mass becomes progressively continental (or inversely maritime) as it travels over land (ocean). The rate of this changes towards continental/maritime conditions is assumed to be a constant fraction (τ) per unit time, i.e. the change in continentality during a time dt is:

$$dC = [-C(1-i_{co}) + (1-C)(i_{co})]\,\tau\,dt \tag{2}$$

with C the continentality (between 0 = sea limit and 1 = land limit), i_{co} = 0 over sea, 1 over land and $\tau\,dt = \tau\,\frac{dx}{dt}\frac{1}{U}dt = \frac{dx/U}{l_0/U_0}\ln(2)$, where dx is the distance traveled by the air mass the time dt, U is the mean wind norm from CLIMBER and l_0/U_0 is the distance/wind ratio corresponding to a continentality change of 2. This ratio is set to $\frac{l_0}{U_0} = \frac{5\ .10^5\,\mathrm{m}}{5\,\mathrm{m/s}}$.

To complete the computation of continentality at a given point, we must first integrate the continentality change over each "incoming air mass path":

$$C_d = \int_{\text{path}} dC = \int_{\text{path}} [-C(1-i_{co}) + (1-C)(i_{co})]\,\frac{\ln(2)/U}{l_0/U_0}\,dx \tag{3}$$

It is necessary to decide the respective weight of each path direction. It is reasonable to rely on simple assumptions: (1) give more weight to path directions which matches the direction of the mean wind, and (2) give zero weight to paths which are in opposition with the mean wind, i.e. penalizing an air-mass traveling against the wind (this would be inconsistent with our above assumptions for the continentality change over a given path). A simple way to perform this is to use the scalar product of the mean wind $\boldsymbol{U}$ and the path direction unit vector $\hat{l}_p$ (integrated over each path):

$$I_d = \int_{\text{path}} \max(\hat{l}_p . \boldsymbol{U}\ ,\ 0) dC \tag{4}$$

The weighted average of the contributions from all paths provides the continentality at the desired point:

$$C = \frac{\sum_d I_d\, C_d}{\sum_d I_d} \tag{5}$$

The last "geographical" variable is the W-slope taking into account (in part) the impact of the mountains on the regional climate. It is computed separately from the continentality indices but in a similar way. Like for continentality, several incoming air masses directions are considered, with the same weighting as before, i.e. through (4). Here, the W-slope corresponds to the mean zonal wind multiplied by the mean east-west slope over approximately 100 km. Only upward trends are retained. That means that the W-slope increases only when the air mass is going up.

Before fitting GAMs, our large-scale data have to be spatially interpolated to the CRU spatial resolution to introduce some spatial variability in CLIMBER outputs. Indeed, because we work on monthly data, no variability is present in the monthly CLIMBER gridcell: for each month, for each available variable, we have only one CRU map and one CLIMBER. This means that for the region associated to one CLIMBER gridcell, we have several CRU gridcells (those contained in the CLIMBER gridcell) and thus several CRU precipitation and temperature values but only one CLIMBER value. This lack of variability does not allow us to apply GAM in favourable conditions. To get one CLIMBER value for each CRU gridcell, the CLIMBER outputs have been bi-linearly

CPD
3, 899–933, 2007
Non-linear statistical downscaling over Europe
M. Vrac et al.

interpolated to the CRU resolution. Hence, the interpolated CLIMBER outputs can be used as predictors of the CRU precipitation and temperatures in GAM.

3.2 Pre-analysis: monthly GAMs

At least two different approaches are conceivable to develop our statistical model: monthly GAMs – i.e. one model per month – or annual GAMs – i.e. one single model calibrated for the data from the 12 months altogether. Although the monthly GAM approach can be used for local projections in a context of "light" climate change (from a few years to a few decades), it is certainly less suitable for long terms (and hence stronger) climate change. Indeed, potential changes and shifts in seasonality would imply that monthly GAMs would be inappropriate and would provide unrealistic downscaled time series. That is why, in order to develop a valid statistical downscaling model for past or future long terms under strong climate change, it has been decided to work on annual GAMs. However, as a pre-analysis, to decide which variables are to be used in the annual GAMs, different models have been developed month by month.

First, for each single available predictor, a GAM is fitted in temperature and in precipitation for each month. Hence, for each month, we can compute the percentage of variance explained by this predictor alone. Figures 2a and b present the results obtained in precipitation and temperature respectively. These figures allow us to explain some seasonal variability for the different variables. For example, while QI can account for a good portion of the temperature variance (Fig. 2b) in the winter months, this variable is less adequate in summer. For precipitation (Fig. 2a), on the opposite, the SLP predictor describes more variance in summer than in winter months.

We can remark that the variables with the lowest percentages of variance explained are the geographical predictors. However, by themselves, these figures alone are not enough to decide which variables are to be kept. Indeed, they present results for GAMs fitted separately for each predictor and do not bring information about GAM fitted to combinations of predictors. To do this, 12 monthly GAMs (one for each month) have been developed for temperatures and precipitation separately.

In order to use the most explicative predictors, each combination of the 15 potential predictors has been tested: if p variables are available, $N=\sum_{k=1}^{p} C_p^k$ combinations are to be tested, where $C_p^k=\frac{p!}{(p-k)!k!}$. With 15 variables, we have N=32 767 combinations for each month. This can appear quite enormous but is actually reasonable in practice since it only performed once. A few hours are enough to fit GAMs for all the combinations. When the N combinations are tested, the "optimal" predictors are selected according to the Bayesian Information Criterion (BIC, Schwartz, 1978):

$$\mathrm{BIC} = \|Y - f(\text{predictors})\|^2 + d \log(n). \quad (6)$$

This criterion combines a term corresponding to a goodness-of-fit measure of the model to the data (the squared term) with a penalty term (last term) depending on the size n of the sample and on the dimension d of the model. The BIC helps to select a model (and therefore the predictors) associated to a good compromise between a model explaining a large percentage of the variance (i.e. with a large number of predictors) and model of reasonable size.

Table 1 gives the percentage of (temperature and precipitation) variance explained by the retained models for four months (January, April, July, and September) representative of the four seasons. Not surprisingly, due to strong nonlinearities and large spatial variability of the rainfall, the percentages of variance are higher for temperatures (from 98.6% in July to 99.5% in September) than for precipitation (from 70% in April to 95% in July).

The number of selected predictors varies from month to month, with, generally, a bigger number for temperatures (from 9 to 12 predictors) than for precipitation (from 5 to 7). Indeed, increasing the number of predictors (i.e. including more predictors) for the precipitation certainly improves the goodness-of-fit to the data but not enough to counterbalance the increase of the penalty term in the BIC.

Among the geographical variables, the altitude (elv) is an important one since it is selected for every monthly model. The advective continentality (Aco) is also regularly chosen for precipitation and temperatures.

To understand the quality of the results brought by these monthly models, we can look, for example, at Figs. 3g–h that present the boxplots of the predicted and observed log-precipitation and temperatures for January (the results are relatively similar for each month).

Boxplots are tools showing the statistical distribution of some sample. The low, medium, and high lines forming the box represent the 25th, 50th, and 75th percentiles (or first, median and third quartiles) respectively, indicating where the central 50% of the data is located. Based on the interquartile range (IQR) calculated by subtracting the first quartile from the third quartile), any data which lies more than 1.5*IQR lower than the first quartile or 1.5×IQR higher than the third quartile is considered as an outlier. The similarity between the predicted and observed statistical distributions in Figs. 3g–h is visually obvious. We remark for precipitation that the very low and very high values are slightly over- and under-predicted respectively. This is logical since, by definition, the GAM approach is developed to model expectation more than extreme behaviours.

Boxplots of the residuals for log-precipitation and temperatures (not shown) show that the residuals (observations - predictions) are well centred around zero, with medians almost exactly at zero and the first and third quartiles very close to the medians. The normal quantile-quantile plots (QQplots, not shown) – i.e. scatterplots of theoretical (Gaussian) quantile vs. observed residuals quantiles, drawn to visually assess the "Gaussianity" of the residuals – display residuals normally distributed for the central values (approximately for quantiles between –2 and +2). Unsurprisingly, a normal distribution is less suitable to characterize the highest and smallest residuals.

In Figs. 3a–c, we compare the observed 3a and predicted 3b precipitation maps and see the map of the residuals 3c for January while Figs. 3d–f display the equivalent maps for temperatures. The map shown in Fig. 3a is obtained by exponentially transforming the log-precipitation predicted by the January GAM model. On both Figs. 3c and f, we can remark some kind of structure for the residuals. For example, a region with negative residuals (i.e. pred > obs) is common at the two variables over the Pyrenees. This is true for any month. In general, the agreements between Figs. 3a and b and between 3d and 3e are clear. The maps and boxplots in Fig. 3 show the high-quality results brought by the monthly GAM approach.

In the following, GAM is not developed month by month but through an annual approach.

3.3 Application: annual GAM to long term downscaling projections

In order to develop our annual GAMs, two types of predictors are first used separately: the physical and the geographical variables. Based on the results obtained from the monthly GAMs in the previous subsection, some variables are disregarded because they were (almost) never retained as predictors or not very informative. For example, although LON is a frequently selected predictor, this variable has not been kept in the following. Indeed, a model based on LON would stay too close from the present climate. No realistic long term downscaling projections could be made based on this variable. Moreover, the splines obtained for LON were generally very flat and close to 0. This means that although LON participated to improve the percentage of variance explained in a present climate, its global contributions were generally relatively small, of the order of the penalty term, and hence LON was not essential to be kept, even in short term future. The same remark holds for Wu for the temperature GAM. Thus, this variable is not retained in the following application.

Hence, the physical predictors retained for the annual GAMs are:

- Q, RH, T, Wu, Wv, Td, DTd, and Ql for the precipitation model and
- Q, RH, SLP, T, Wv, Td, DTd, and Ql for the temperature one.

These predictors, when combined altogether, are supposed to have the highest percentage of variance explained (among the physical variables) for the whole year. The geographical variables retained are the same for the precipitation and temperature

CPD
3, 899–933, 2007
Non-linear statistical downscaling over Europe
M. Vrac et al.

annual GAMs and are: the altitude (elv), the advective continentality (Aco) and the W-slope (Wsl).

First, the (precipitation and temperatures) physically-based and geographically based annual GAMs are calibrated. The geographical predictors explain 17.5% and 79% of variance for log-precipitation and temperatures respectively, while the physical ones explain 60% and 91% of variance for log-precipitation and temperatures respectively.

Figures 4 and 5 show the associated residuals (obs-predicted) for the four months (January, April, July, and October), respectively for the log-precipitation with geographical predictors (Figs. 4a–d) and with physical predictors (Figs. 4e–h), and for the temperatures with geographical predictors (Figs. 5a–d) and with physical predictors (Figs. 5e–h).

Although with a relatively low percentage of variance explained (17.5%), the log-precipitation residuals maps obtained from the geographical variables are actually quite acceptable. This low percentage of variance comes from some relatively small errors distributed over the year and by stronger residuals (meaning stronger errors) in Southern Europe in July and August. Precipitation predictions (Fig. 4) seem to be slightly better with physical variables than with geographical ones, overall for summer months. This is true also for temperatures (Fig. 5): despite systematic errors of about 5°C over high mountains, physical variables look more efficient to provide local predictions whose the residuals are close to 0.

However, these differences between physically- and geographically-based predictions are slight and are not informative about the behaviour of the predictions in the context of a different climate.

In order to test the annual models for climate different from the one used for calibration, we downscale the large-scale CLIMBER data over two regions corresponding approximately to North America (USA and Canada) and Northern Europe (with a part of Siberia). The North America results of residuals (obs – pred) are presented for (log) precipitation in Figs. 6a–d and in Figs. 6e–h for temperatures, from the geographical predictors. The results from the physical predictors and Northern Europe results are not shown here but are discussed in the following.

North America precipitation residuals maps from the geographical variables (Figs. 6a–d) show coherent spatial structures, despite more or less pronounced residuals (from –6 to +2 units). The equivalent maps from the physical predictors (not shown) are associated to larger residuals (comprised between –30 and –15 units) and to very unrealistic structures. The latter can be explained by the values of the physical predictors that are out of the calibration range observed over Western Europe. Moreover, in Figs. 6a–d, the downscaled precipitation is associated to larger errors inland than along the East and West American coasts: the continentality index seems to play a non-negligible role. Furthermore, we can remark that the residuals are weaker for summer than for winter months.

The same conclusions hold for the precipitation projections over the Northern Europe region (not shown): residuals maps with unrealistic structures from physical predictors (out of the calibration range) and with coherent spatial structures from geographical variables; weaker residuals with geographical (–5 to +2 units) than physical variables (–30 to –10 units); the geographical predictors provide smaller errors inland than along the coasts; weaker in summer then in winter.

Figures 6e–h for the North America temperature residuals maps show similar results than previously despite some differences. The similarities are obvious: unrealistic maps from physical predictors (not shown) with high residuals (+120°C to +220°C) and continuous aspect maps from the geographical variables with lower residuals (–30°C to +10°C), as previously, smaller in summer. The inland/coasts differences visible for precipitation are not present for temperatures. The differences are more pronounced according to the latitudes: for example, in January, north is associated to large residuals, and the more we go south, the smaller the errors. The Northern Europe temperature results (not shown) are equivalent except for the latitudes-driven residuals. Indeed, while residuals seem to be latitudes-driven in summer, the residuals structures are longitudinal in winter (with relatively small values).

In general, we see that the geographical predictors are more "robust" than physical variables in downscaling precipitation and temperature values under large-scale climate conditions strongly different from the calibration ones.

Based on these results, annual GAMs are fitted to present climate Western Europe temperatures and precipitation, and used to deduce last glacial maximum (LGM, 21ky) temperatures and precipitation. For this LGM downscaling, the retained predictors are the geographical variables (elv, Aco, and Wsl), where one physical predictor is added, chosen from the previous plots and analyses. For precipitation, this variable is the CLIMBER sea level pressure (SLP), while for temperatures it is the CLIMBER temperature (T). Indeed, although the geographical predictors bring robustness to the downscaling process, they are not sufficient by themselves to drive correctly the local variables. The selected added variables are supposed to provide useful large-scale information in order to have more physically-driven temperatures and precipitation. As the LGM sea level is 120 m lower than today, the LGM elv predictor is taken as the present altitude plus 120 meters. Note that the ice sheets supposed to cover northern Europe are not modelled in this work.

The monthly precipitation maps of the relative differences with respect to present precipitation are presented in Figs. 7a–d and the monthly temperature maps of the absolute differences with respect to present temperatures are presented in Figs. 7e–h, for January, April, July, and October.

Figures 7a–d show that, in general, LGM climate is drier that present one. However, regionally, some increases of the precipitation are to be noted. Moreover, the North-East part of the studied region presents a clear increase, whatever the month.

For temperatures in Figs. 7e–h, as expected, we see that the LGM climate is colder that present, whatever the month and the region. A latitudinal effect is discernible for about November-May (not shown completely, see January), with stronger differences in Northern regions and smaller ones in South. LGM June–October show more uniform differences with respect to present with somehow a "coastal" effect, see for example July.

In order to have more assessment of the LGM results brought by our CLIMBER-driven GAM, reconstructed LGM precipitation and temperature data have been compared to our downscaled values. These data are local reconstructions from pollen data using inverse vegetation modeling (Wu et al., 2007). The locations of the 10 points in Western Europe are shown on Fig. 8. Moreover, four GCMs involved in the Paleoclimate Modelling Intercomparison Project II (PMIP2, e.g. Kageyama et al., 2006; Ramstein et al., 2007) are also used: MIROC3.2.2, FGOALS-1.0g, IPSL-CM4-V1-MR, and HadCM3M2. These fully coupled atmosphere-ocean GCM experiments are available in the PMIP2 database as of 7 April 2007 (http://pmip2.lsce.ipsl.fr). Hence, for each of the 10 locations, we have:

1. the LGM reconstructed temperature and precipitation values (min, median, and max)

2. the temperature and precipitation values for the CLIMBER grid-cells containing the points,

3. the projections obtained from the CLIMBER-driven GAM,

4. the four (temp. and precipitation) GCMs values for the model grid-cells containing the points.

For each of these 10 locations, we compare these different values for LGM January and July in Figs. 9a–b for temperature and in Figs. 9c–d for precipitation. Note that the CLIMBER precipitation simulations are not used in GAM for downscaling and are only provided here for comparisons.

Although the goal of this paper is not to assess the CLIMBER simulations, the most surprising result may be the good agreement between CLIMBER and the local reconstructions. For both temperature and precipitation, the GAM downscaled values are realistic and generally brought some useful additional information. Indeed, even when CLIMBER is far away from the values to be retrieved/approximated, the downscaling process is sometimes capable of moving away from CLIMBER and getting closer to the reconstructions. For example, for July precipitation (Fig. 9d), in station 10 (the right one), CLIMBER precipitation is clearly to large and the downscaled value is brought back to the low part of the GCMs range, closer to the reconstructed precipitation. A counterexample is given by stations 8 and 9 (in the same Fig. 9d), where CLIMBER precipitation is too high and the downscaled value is higher. This result is not surprising since these stations are the two locations over Italy where we see, in Fig. 7c, an unrealistic increase of precipitation larger than 100%.

For temperatures, the results are generally better for January than for July. The PMIP2 GCMs used in this work give ranges of temperatures quite far from the reconstructions. Hence, as the CLIMBER temperatures are close to the GCMs range, although the CLIMBER-driven GAM downscaled temperatures are capable of moving away from the CLIMBER values, the downscaled temperatures tend to stay distant from "real" values.

As a summary of these results, Table 2 presents the mean temperatures (in °C) and mean precipitation (in mm/month) computed for January and July from the 10 stations and without stations 8 and 9 from the reconstructed data, the GCMs and the GAM projections. We see that in general the mean GAM downscaled values are closer to the reconstructions than the PMIP2 GCMs. However, due to stations 8 and 9 with too large downscaled precipitation, for the July mean precipitation, the GCMs are closer than the downscaled data. By removing these two stations for the mean computation, the GAM approach gives us a mean value close to the one from the reconstructions.

In general, the CLIMBER-driven GAM based downscaling process provides satisfying local temperatures and precipitation, thus showing the quality of the proposed method.

4 Conclusions and discussion

In this article, we developed a statistical downscaling method allowing a non-linear modeling of the relationships between large and small scales. In this context of downscaling – indispensable in any impacts studies and often required in paleoclimate researches – the Generalized Additive Model (GAM) developed here represents an original approach.

Monthly GAMs (i.e. calibration month by month) can be used in a framework of slightly changed climate conditions, for short terms local projections (from a few years to some decades). However, in a (past or future) long terms climate change framework, annual GAMs (i.e. calibration for the 12 months altogether) are preferable. Indeed, they allow avoiding potential errors due to climate change associated to seasonal shifts and changes that would prevent us from using monthly models.

The GAM calibrations for temperatures and precipitation according to two types of predictors (physical and geographical predictors), as well as the CLIMBER-driven local projections for different regions of the world (Western Europe, North America, Northern Europe) have shown that the geographical predictors provide robustness to the downscaling process. While the physical variables alone seem to be unusable for projections when the predictors are out of the calibration range, the physical ones are steadier and bring some stability and robustness to the downscaling projections. These results show, for a part, the limitation of any statistical downscaling method when the predictors (GCM outputs) used for projections come out of the domain on which the model has been calibrated. Hence, physical predictors have to be chosen carefully, and to be associated with geographical variables for realistic projections.

Based on the geographical predictors (altitude, advective continentality, and W-slope) associated with physical one selected with care (CLIMBER Temp for temperatures and CLIMBER SLP for precipitation), annual GAMs have been calibrated on present climate and used for local projections at the LGM. Although we have some regional increase, the resulting maps showed realistic decreases in temperature and precipitation with respect to present climate, at least over France, i.e. the central part of the Western Europe region. When compared to reconstructed temperature and precipitation values and simulations from four GCMs involved in PMIP2, the downscaled values behave well, showing that CLIMBER-driven GAMs are an efficient approach to provide plausible LGM projections of local temperatures and precipitation.

As a perspective, it would be interesting to use the couple CLIMBER/GAM approach to generate long time series (e.g. thousand years or more) of local variables such as temperatures and precipitation. The produced data would be useful to understand the past climate evolution and could be compared to time series reconstructed from proxies.

It would also be worth calibrating and applying the GAM approach to the GCMs involved in PMIP2 instead of the CLIMBER model. Based on their resolution higher than the CLIMBER resolution, we can expect more precise results. Moreover, we would dispose of a large set of downscaled values, expressing the local variability of the projections and opening ways for more comparisons and research.

Acknowledgements. Although this work has been funded in part by the Agence Nationale pour la gestion des Déchets RAdioactifs (ANDRA), it has not been subjected to the Agency's required peer and policy review and therefore does not necessarily reflect the views of the Agency, and no official endorsement should be inferred.

We acknowledge the international modeling groups for providing their data for analysis, the Laboratoire des Sciences du Climat et de l'Environnement (LSCE) for collecting and archiving the model data. We also acknowledge H. Wu for providing the reconstruction data.

The PMIP2/MOTIF Data Archive is supported by CEA, CNRS, the EU project MOTIF (EVK2-CT-2002-00153) and the Programme National d'Etude de la Dynamique du Climat (PNEDC). The analyses were performed using version 06-04-2007 of the database. More information is available on http://www-lsce.cea.fr/pmip/ and http://www-lsce.cea.fr/motif/.

This work was supported by the European E2-C2 grant, the National Science Foundation (grant: NSF-GMC (ATM-0327936)) and the ANR-AssimilEx project.

The authors would also like to credit the contributors of the R project. The GAM fitting has been realized through the R software with the package "mgcv" downloadable on the R project for statistical computing website (http://www.r-project.org/).

References

Bardossy, A., Muster, H., Duckstein, L., and Bogardi, I.: Automatic classification of circulation patterns for stochastic precipitation modelling. Stochastic and Statistical Methods in Hydrology and Environmental Engineering, 1. Extreme Values: Floods and Droughts, 1994.

de Boor, C.: A Practical Guide to Splines. Springer Series: Applied Mathematical Sciences, Vol. 27 1st ed. 1978. 1st hardcover printing, XVIII, 372 p. ISBN: 978-0-387-95366-3, 2001.

Charles, S. P., Bates, B. C., Whetton, P. H., and Hughes, J. P.: Validation of downscaling models for changed climate conditions: case study of southern Australia, Clim. Res., 12, 1–14, 1999.

Hastie, T. J. and Tibshirani, R. J.: Generalized Additive Models. Chapman and Hall, 1990.

Huth, R.: Disaggregating climatic trends by classification of circulation patterns, Int. J. Climatol., 21, 135–153, 2001.

Huth, R.: Statistical downscaling of daily temperature in central europe, J. Climate, 15, 1731–1742, 2002.

Kageyama, M., Peyron, O., Pinot, S., Tarasov, P., Guiot, J., Joussaume, S., and Ramstein, G.: The Last Glacial Maximum climate over Europe and western Siberia: a PMIP comparison between models and data, Clim. Dynam., 17, 23–43, 2001.

Kageyama, M., Laîné, A., Abe-Ouchi, A., Braconnot, P., Cortijo, E., Crucifix, M., de Vernal, A., Guiot, J., Hewitt, C. D., Kitoh, A., Kucera, M., Marti, O., Ohgaito, R., Otto-Bliesner, B., Peltier, W. R., Rosell-Melé, A., Vettoretti, G., Weber, S. L., and Yu, Y.: MARGO Project Members. Last Glacial Maximum temperatures over the North Atlantic, Europe and western Siberia: a comparison between PMIP models, MARGO sea–surface temperatures and pollen-based reconstructions, Quat. Sci. Rev., 25, 2082–2102, 2006.

Katz, R. W.: Techniques for estimating uncertainties in climate change scenarios and impact studies, Clim. Res., 20, 167–185, 2002.

Liang, X.-Z., Pan, J., Zhu, J., Kunkel, K. E., Wang, J. X. L., and Dai, A.: Regional climate model downscaling of the u.s. summer climate and future change, J. Geophys. Res., 111, D10108, doi:101029/2005JD006685, 2006.

New, M., Lister, D., Hulme, M., and Makin, I.: A high-resolution data set of surface climate over global land areas, Clim. Res., 21, 1–25, 2002.

Petoukhov, V., Ganopolski, A., Brovkin, V., Claussen, M., Eliseev, A., Kubatzki, C., and Rahmstorf, S.: CLIMBER-2: a climate system model of intermediate complexity, Clim. Dynam., 16,

1–17, 2000.
Petoukhov, V., Claussen, M., Berger, A., Crucifix, M., Eby, M., Eliseev, A. V., Fichefet, T., Ganopolski, A., Goosse, H., Kamenkovich, I., Mokhov, I. I., Montoya, M., Mysak, L. A., Sokolov, A., Stone, P., Wang, Z., and Weaver, A. J.: EMIC Intercomparison Project (EMIP–CO2): comparative analysis of EMIC simulations of climate, and of equilibrium and transient responses to atmospheric CO2 doubling, Clim. Dynam., 25, 363–385, 2005.
Rahmstorf, S. and Ganopolski, A.: Long-Term Global Warming Scenarios Computed with an Efficient Coupled Climate Model, Climatic Change, 43, 353–367, 1999.
Ramstein, G., Kageyama, M., Guiot, J., Wu, H., Hély, C., Krinner, G., and Brewer, S.: How cold was Europe at the Last Glacial Maximum? A synthesis of the progress achieved since the first PMIP model-data comparison, Clim. Past. Discuss., 3, 1–24, 2007.
Schwartz, G.: Estimating the dimension of a model, The Annals of Statistics, 6, 461–464, 1978.
Snell, S. E., Gopal, S., and Kaufmann, R. K.: Spatial interpolation of surface air temperatures using artificial neural networks: Evaluating their use for downscaling GCMs, J. Climate, 13, 886–895, 2000.
Vrac, M. and Naveau, P.: Stochastic downscaling of precipitation: From dry events to heavy rainfalls, Water Resour. Res., 43, W07402, doi:10.1029/2006WR005308, 2007.
Vrac, M., Stein, M., and Hayhoe, K.: Statistical downscaling of precipitation through a non-homogeneous stochastic weather typing approach, Climate Res., in press, 2007a
Wilby, R. L., Wigley, T. M. L., Conway, D., Jones, P. D., Hewitson, B. C., Main, J., and Wilks, D. S.: Statistical downscaling of general circulation model output: A comparison of methods, Water Resour. Res., 34, 2995–3008, 1998.
Wilks D. S. and Wilby, R. L.: The weather generation game: a review of stochastic weather models, Progress in Physical Geography, 23, 329–357, 1999.
Wilks, D. S.: Multisite downscaling of daily precipitation with a stochastic weather generator, Clim. Res., 11, 125–136, 1999.
Wood, A. W., Leung, L. R., SRidhar, V., and Lettenmaier, D. P.: Hydrologic implications of dynamical and statistical approaches to downscaling climate model outputs, Clim. change, 62, 189–216, 2004.
Wu, H., Guiot, J., Brewer, S., and Guo, Z.: Climatic changes in Eurasia and Africa at the last glacial maximum and mid-Holocene: reconstruction from pollen data using inverse vegetation modelling, Clim. Dyn., doi:10.1007/s00382-007-0231-3, 2007.

Zorita, E. and von Storch, H.: The analog method as a simple statistical downscaling technique: Comparison with more complicated methods, J. Climate, 12, 2474–2489, 1998.

Table 1. Percentages of (temperature and precipitation) variance explained by the retained models for four months (January, April, July, and September) representative of the four seasons.

Months	% of temperature variance explained	% of precipitation variance explained
JANUARY	99%	79%
APRIL	99.3%	70%
JULY	98.6%	95%
SEPTEMBER	99.5%	85.3%

Table 2. Mean temperatures (in °C) and precipitation (in mm/month) computed for January and July from the 10 stations and without stations 8 and 9.

		From the 10 stations	without stations 8 and 9
January mean temperatures	from reconstructions	–8.7	–9.3
	from GCMs	–0.3	–0.3
	from GAM	–3	–3.4
July mean temperatures	from reconstructions	–2.5	–3.2
	from GCMs	14.2	13
	from GAM	10.6	9.9
January mean precipitation	from reconstructions	61.4	59.6
	from GCMs	85.7	91.2
	from GAM	54.4	62.1
July mean precipitation	from reconstructions	35.3	40.1
	from GCMs	39.7	45.9
	from GAM	49.2	43.4

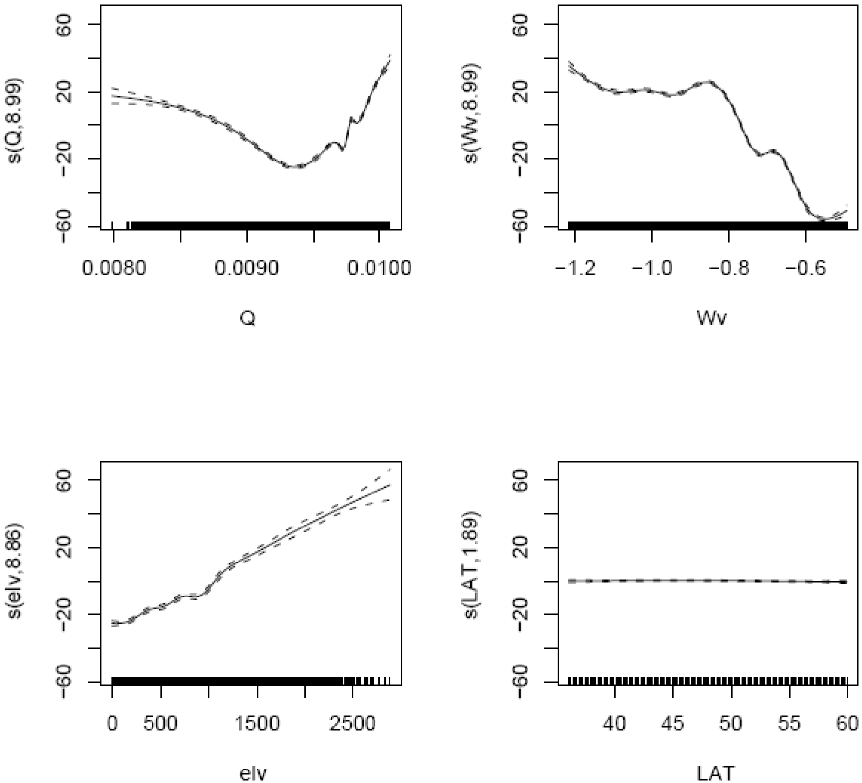

Fig. 1. Spline functions estimated for a toy model calibrated for the July CRU precipitation data with predictors Q, Wv, elv, and LAT. While the contributions from Q and Wv are modeled through strong non-linearity, elv and LAT contributions are mostly linear, and the LAT spline is clearly uninformative in this toy model.

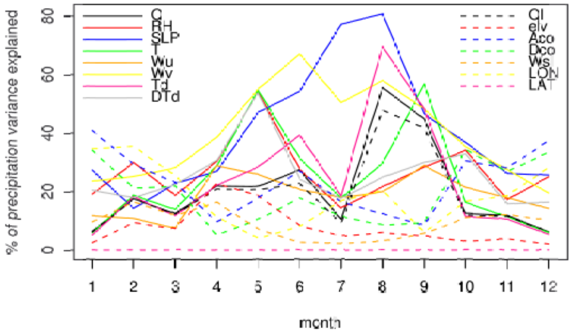

(a) Percentage of precipitation variance

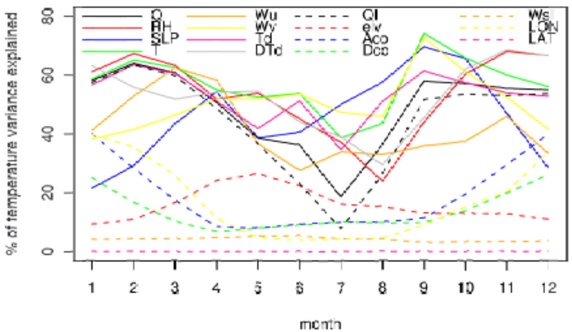

(b) Percentage of temperature variance

Fig. 2. Percentage of **(a)** precipitation and **(b)** temperature variance explained for each month by each predictor separately.

CPD

3, 899–933, 2007

EGU

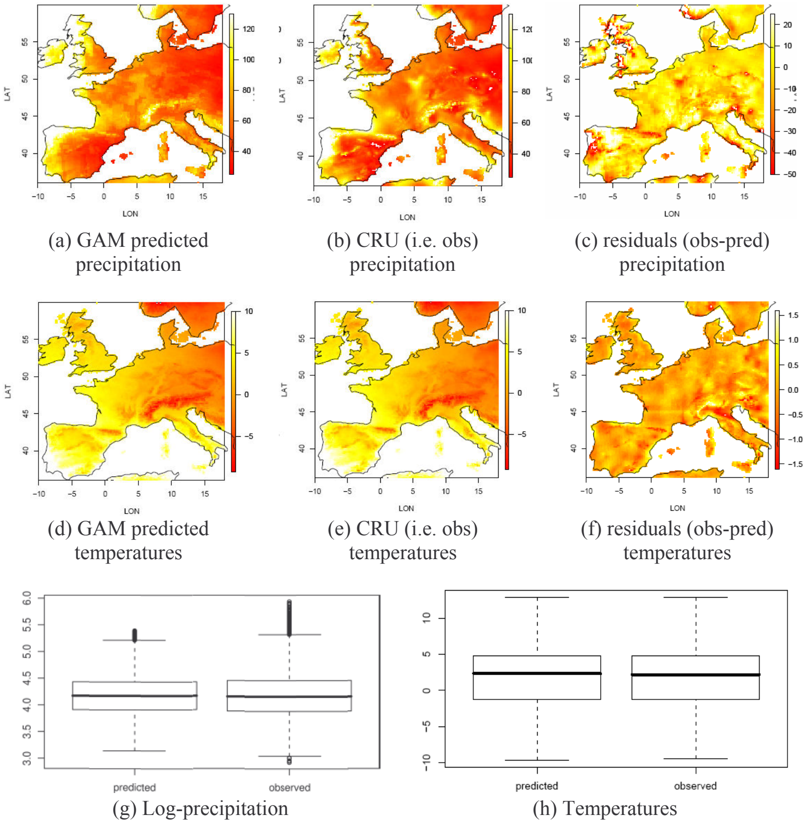

Fig. 3. January maps of **(a)** exponential of GAM predicted precipitation, **(b)** observed precipitation, **(c)** precipitation residuals (i.e. b–a), **(d)** GAM predicted temperatures, **(e)** observed temperatures, and **(f)** temperature residuals (i.e. d–e); and associated boxplots of the predicted and observed **(g)** log-precipitation and **(h)** temperatures (the results are relatively similar for every month). Predictions were obtained from the monthly January (temperature or precipitation) GAMs.

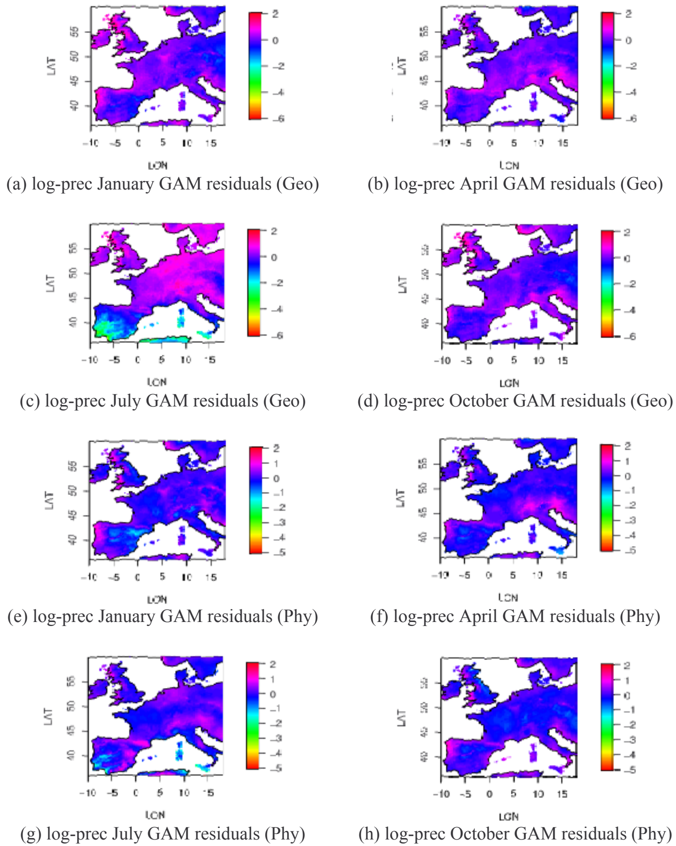

(a) log-prec January GAM residuals (Geo) (b) log-prec April GAM residuals (Geo)

(c) log-prec July GAM residuals (Geo) (d) log-prec October GAM residuals (Geo)

(e) log-prec January GAM residuals (Phy) (f) log-prec April GAM residuals (Phy)

(g) log-prec July GAM residuals (Phy) (h) log-prec October GAM residuals (Phy)

Fig. 4. Log-precipitation GAM residuals (obs-pred) maps for Western Europe, (**a**–**d**) from the geographical predictors, (**e**–**h**) from the physical predictors, for January, April, July, and October respectively. Predictions were obtained from annual (i.e. 12 months together) Western Europe log-precipitation GAMs.

CPD

3, 899–933, 2007

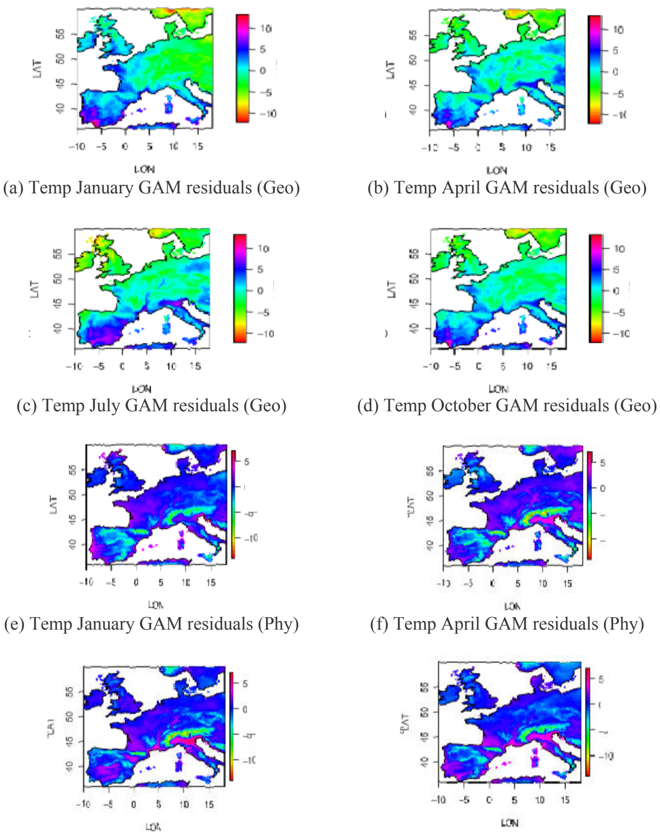

(a) Temp January GAM residuals (Geo)
(b) Temp April GAM residuals (Geo)
(c) Temp July GAM residuals (Geo)
(d) Temp October GAM residuals (Geo)
(e) Temp January GAM residuals (Phy)
(f) Temp April GAM residuals (Phy)
(g) Temp July GAM residuals (Phy)
(h) Temp October GAM residuals (Phy)

Fig. 5. Temperature GAM residuals (obs-pred) maps for Western Europe, (**a**–**d**) from the geographical predictors, (**e**–**h**) from the physical predictors, for January, April, July, and October respectively. Predictions were obtained from annual (i.e. 12 months together) Western Europe temperature GAMs.

CPD

3, 899–933, 2007

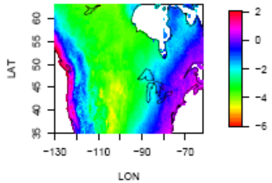

(a) Log-prec January GAM residuals (Geo)

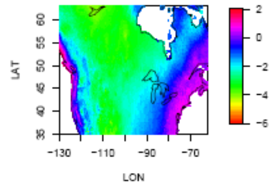

(b) Log-prec April GAM residuals (Geo)

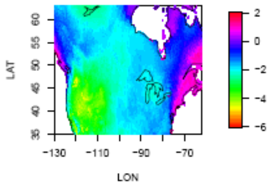

(c) Log-prec July GAM residuals (Geo)

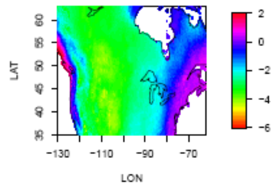

(d) Log-prec October GAM residuals (Geo)

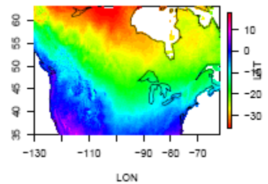

(e) Temp January GAM residuals (Geo)

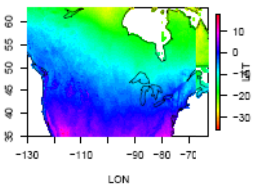

(f) Temp April GAM residuals (Geo)

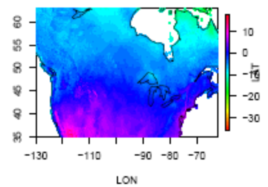

(g) Temp July GAM residuals (Geo)

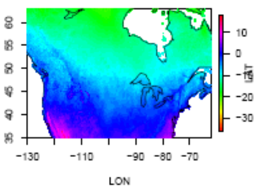

(h) Temp October GAM residuals (Geo)

Fig. 6. (**a**–**d**) Log-precipitation and (**e**–**h**) temperature GAM residuals (obs-pred) maps for North America, from the geographical predictors, for January, April, July, and October respectively. Predictions were obtained from annual Western Europe GAMs.

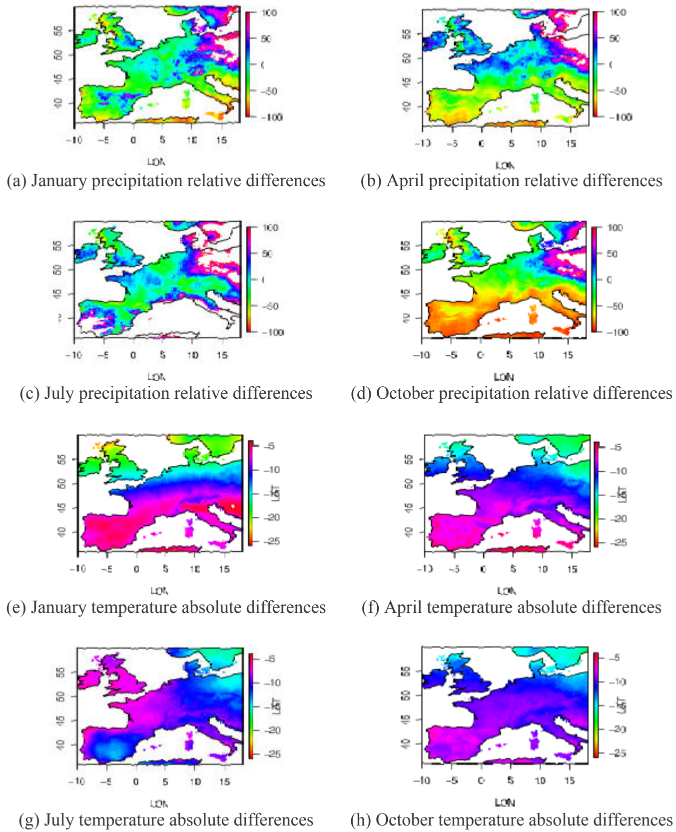

(a) January precipitation relative differences (b) April precipitation relative differences

(c) July precipitation relative differences (d) October precipitation relative differences

(e) January temperature absolute differences (f) April temperature absolute differences

(g) July temperature absolute differences (h) October temperature absolute differences

Fig. 7. Monthly maps of (**a–d**) relative differences and (**e–h**) absolute differences (with respect to present) between GAM downscaled LGM values (from geographical predictors and CLIMBER SLP for precipitation and from geographical predictors and CLIMBER T for temperatures) and present (a–d) precipitation and (e–h) temperatures for January, April, July, and October respectively. Predictions were obtained from annual Western Europe GAMs.

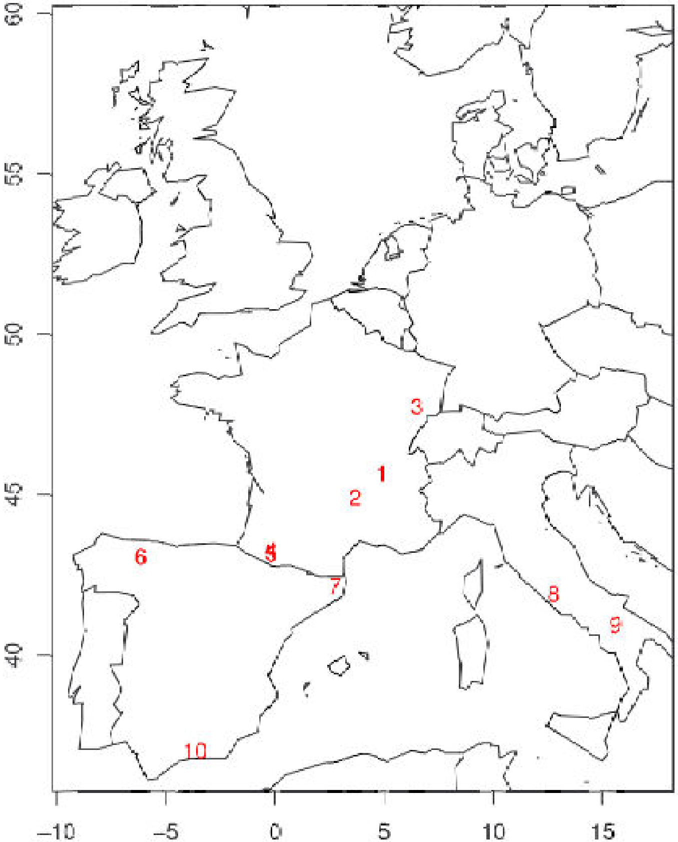

Fig. 8. Locations of the 10 reconstructed LGM data in Western Europe whose the values have to be compared to our GAM downscaled values.

CPD
3, 899–933, 2007

Non-linear statistical downscaling over Europe

M. Vrac et al.

EGU

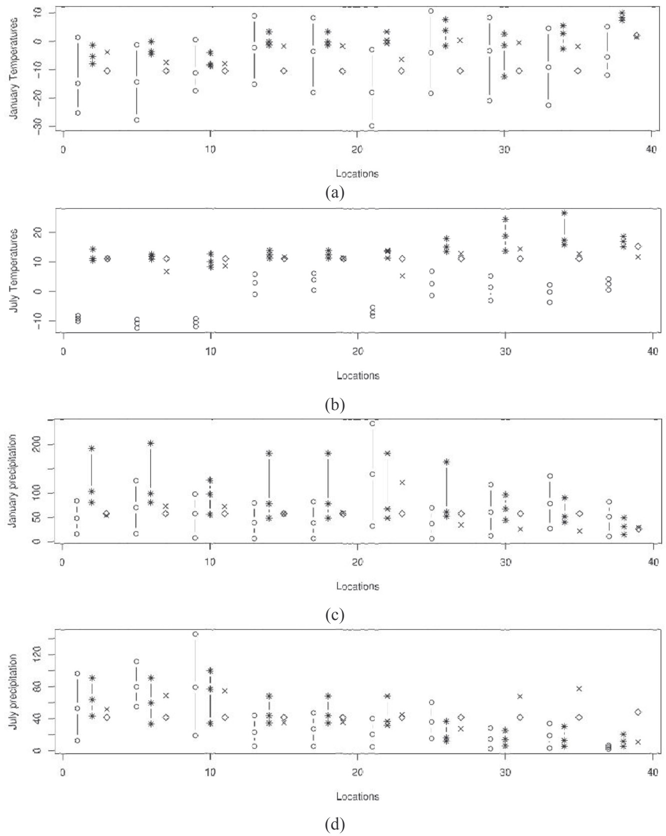

Fig. 9. (**a**–**b**) Comparison at the 10 locations of the reconstructed temperatures (min, median, and max in o signs), the min, median, and max temperature values (in asterisk signs) from the four GCMs grid-cell (containing the location), the CLIMBER grid-cell (containing the location) temperatures (in diamond signs), and the CLIMBER-driven GAM downscaled temperatures (in × signs); (a) in January, (b) in July; (**c**–**d**) idem for precipitation values.

CPD

3, 899–933, 2007

Title Page
Abstract | Introduction
Conclusions | References
Tables | Figures
◀| |▶
◀ ▶
Back | Close
Full Screen / Esc
Printer-friendly Version
Interactive Discussion

EGU